The EMBO Journal (2012) 31, 2566–2578 | © 2012 European Molecular Biology Organization | Some Rights Reserved 0261-4189/12
www.embojournal.org

THE EMBO JOURNAL

EMBO open

Co-transcriptional degradation of aberrant pre-mRNA by Xrn2

Lee Davidson, Alastair Kerr and Steven West*

Wellcome Trust Centre for Cell Biology, University of Edinburgh, Edinburgh, UK

Eukaryotic protein-coding genes are transcribed as pre-mRNAs that are matured by capping, splicing and cleavage and polyadenylation. Although human pre-mRNAs can be long and complex, containing multiple introns and many alternative processing sites, they are usually processed co-transcriptionally. Mistakes during nuclear mRNA maturation could lead to potentially harmful transcripts that are important to eliminate. However, the processes of human pre-mRNA degradation are not well characterised in the human nucleus. We have studied how aberrantly processed pre-mRNAs are degraded and find a role for the 5′→3′ exonuclease, Xrn2. Xrn2 associates with and co-transcriptionally degrades nascent β-globin transcripts, mutated to inhibit splicing or 3′ end processing. Importantly, we provide evidence that many endogenous pre-mRNAs are also co-transcriptionally degraded by Xrn2 when their processing is inhibited by Spliceostatin A. Our data therefore establish a previously unknown function for Xrn2 and an important further aspect of pre-mRNA metabolism that occurs co-transcriptionally.

The EMBO Journal (2012) **31,** 2566–2578. doi:10.1038/emboj.2012.101; Published online 20 April 2012
Subject Categories: RNA
Keywords: transcription; RNA processing; RNA degradation

Introduction

Eukaryotic pre-mRNA transcripts are synthesised by RNA polymerase II (Pol II). They are matured by capping, splicing and 3′ end cleavage and polyadenylation before the mRNA is exported into the cytoplasm and translated (Moore and Proudfoot, 2009). *In vivo*, most processing is thought to occur co-transcriptionally via the recruitment of pre-mRNA processing factors to the c-terminal domain (CTD) of the large subunit of RNA polymerase II (Pol II) (Buratowski, 2009). This is at least in part governed by phosphorylation of serines 2, 5 and 7 within the CTD heptapeptide repeat sequence, YSPTSPS (Bentley, 2005; Corden, 2007; Kim *et al*, 2010; Schwer and Shuman, 2011). Most human pre-mRNAs contain multiple exons separated by much larger intron sequences and more than 90% may be alternatively spliced or 3′ end processed to produce multiple mRNA isoforms (Wang *et al*, 2008; Ozsolak *et al*, 2010).

Although productive processing is frequently transcription coupled, other potentially co-transcriptional aspects of mRNA metabolism and biogenesis have not been explored in detail. Recent studies indicated that transcripts deriving from mutant gene templates are retained at or close to their site of synthesis implying that degradation was occurring there (Custodio *et al*, 1999; de Almeida *et al*, 2010; Martins *et al*, 2011). However, other blocks to splicing cause some transcripts to accumulate in the nucleoplasm or even, in the case of some budding yeast transcripts, in the cytoplasm (Hilleren and Parker, 2003; Kaida *et al*, 2007; Brody *et al*, 2011; Martins *et al*, 2011). Although temporal and spatial aspects of decay are not well understood, many exonucleolytic enzymes that execute degradation are well defined.

The exosome plays a major role in pre-mRNA turnover in eukaryotes. It is a multi-protein complex where 3′→5′ exonuclease activity is provided by its Rrp44/Dis3 subunit and Rrp6 co-factor (Dziembowski *et al*, 2007; Schmid and Jensen, 2008). Interestingly, Rrp44/Dis3 also possesses endonuclease activity (Lebreton *et al*, 2008; Schneider *et al*, 2009). Loss of *S. cerevisiae* exosome function stabilises transcripts that are splicing or 3′ end processing defective (Bousquet-Antonelli *et al*, 2000; Torchet *et al*, 2002). The budding yeast exosome is also required for the retention of some aberrant mRNAs at their site of synthesis (Hilleren *et al*, 2001). Similarly, depletion of the human homologue of Rrp6 (hRrp6) causes β-globin transcripts carrying deletions or mutations in intron 2 to be released from their site of synthesis (de Almeida *et al*, 2010; Eberle *et al*, 2010). In Drosophila the exosome has been found associated with the Pol II elongation factor Spt5 and with nascent mRNPs highlighting the possibility that surveillance is co-transcriptional (Andrulis *et al*, 2002; Hessle *et al*, 2009).

Human and *S. cerevisiae* nuclei also contain 5′→3′ exonucleases: Xrn2 and Rat1 respectively. Xrn2 and Rat1 degrade the Pol II associated product of poly(A) site cleavage, which is important for Pol II termination (Kim *et al*, 2004; Gromak *et al*, 2006). In the case of the human β-globin gene, co-transcriptional cleavage of terminator transcripts generates entry sites for Xrn2 (West *et al*, 2004). Xrn2 is also involved in processing and degradation of many ribosomal RNAs (Wang and Pestov, 2010). Other functions of Rat1 include degradation of some splice defective pre-mRNAs (Bousquet-Antonelli *et al*, 2000), transcripts that fail to acquire a cap (Jimeno-Gonzalez *et al*, 2010), RNA transcribed from telomeric repeats (Luke *et al*, 2008) and promoting transcriptional termination of Pol I (El Hage *et al*, 2008; Kawauchi *et al*, 2008).

We have examined mechanisms used for degrading aberrant transcripts as well as their timing with relation to transcription. Analysis of nascent transcripts provides strong evidence that degradation of β-globin pre-mRNA blocked in

*Corresponding author. Wellcome Trust Centre for Cell Biology, University of Edinburgh, Michael Swann Building, King's Buildings, Mayfield Road, Edinburgh, EH9 3JR, UK. Tel: +44 131 650 7110; Fax: +44 131 650 5379; E-mail: steven.west@ed.ac.uk

Received: 26 September 2011; accepted: 27 March 2012; published online 20 April 2012

splicing or 3′ end processing is co-transcriptional. Similar to previous reports we find a role for the exosome in degrading some aberrant β-globin transcripts but also find that the 5′→3′ exonuclease Xrn2 binds to aberrant β-globin transcripts that are stabilised by its depletion. Some nascent endogenous pre-mRNA transcripts are also stabilised by Xrn2 depletion following use of the splicing inhibitor, Spliceostatin A. These data indicate that co-transcriptional degradation of RNA is an important means of exerting quality control on transcription.

Results

To begin to study the degradation of aberrant pre-mRNA, we used five plasmids containing different versions of the human β-globin gene each driven by the HIV promoter (Figure 1A). These were an unmodified wild type (WT) gene, one with a mutated 3′ splice site in intron 1 (In1m), one with a mutant poly(A) site (pAm), as well as versions of In1m and pAm lacking the 3′ flanking sequence necessary for termination (ΔTIn1m and ΔTpAm). These constructs enabled us to assay the implications of splicing and 3′end processing failure and any additional effect of the terminator sequence, which is known to be important for efficient mRNA production (West and Proudfoot, 2009).

We first assayed for β-globin RNA levels from each construct. HeLa cells were transfected with each β-globin plasmid and a construct containing the Pol III transcribed VA gene, which acts as a control for equivalent transfection efficiency. Total RNA was then isolated and reverse transcribed using random hexamers. To detect all processed and unprocessed forms of β-globin RNA, cDNA was real time PCR amplified using primers directed to exon 3 (Figure 1B). Following correction to VA transcript levels, we observed fewer β-globin transcripts in samples from cells transfected with mutant constructs when compared to the WT suggesting that the mutations somehow inhibit β-globin RNA production. One way that this could be achieved is through reduced transcription. However, transcription of these plasmids has been analysed previously where it was found to be reduced only up to 2-fold (Dye and Proudfoot, 1999; Dye and Proudfoot, 2001). Since the reduction in RNA that we observe is much greater than that, particularly for ΔTIn1m, pAm and ΔTpAm, we hypothesised that many mutant transcripts were being degraded, possibly as a result of impaired processing.

To understand more about the effects of the mutations on pre-mRNA processing, we next assayed total RNA from the same samples using Northern blotting with a probe directed to exon 3 (Figure 1C). To control for transfection variance we analysed RNA from a co-transfected plasmid expressing erythropoietin (EPO). We observed a strong band corresponding to β-globin mRNA in the WT sample. In contrast, much weaker bands were observed in In1m and ΔTIn1m samples, which were larger owing to intron 1 inclusion caused by the mutated splice site. No obvious product was detected in pAm and ΔTpAm samples. These data confirm that the intron 1 and pA mutations prevent the accumulation of any correctly processed β-globin mRNA. Additional real-time PCR data confirmed the inhibitory effects of the mutations on splicing and 3′ end processing (Supplementary Figure 1).

The data so far show that the mutations employed here prevent β-globin mRNA accumulation and reduce the overall level of β-globin RNA detectable in the total RNA fraction. For a more detailed insight into RNA production from mutant templates, we analysed transcripts from each β-globin gene in three different cellular fractions. We used a well characterised technique to isolate chromatin-associated, nucleoplasmic and cytoplasmic RNA from HeLa cells transfected with each β-globin plasmid and the EPO control plasmid (Wuarin and Schibler, 1994). To detect the full range of transcripts, each sample was analysed by Northern Blotting using the β-globin exon 3 probe (Figure 1D). In the chromatin fraction, we observed a band representing spliced β-globin in WT samples but no predominant species in any other sample. A lack of product indicates that mutant RNA is either not produced, is very unstable or does not accumulate sufficient amounts of any distinct species to be detected by Northern analysis. A strong band corresponding to mature β-globin mRNA was observed in nucleoplasmic and cytoplasmic WT samples. Much fainter bands were seen in nucleoplasmic and cytoplasmic In1m and ΔTIn1m samples corresponding to RNA retaining intron 1. Very little pAm or ΔTpAm product was detected. The observation that only spliced and 3′ end processed RNA predominates in nucleoplasmic and cytoplasmic fractions is consistent with the idea that pre-mRNA processing occurs before transcripts are released from chromatin (Dye *et al*, 2006).

We wished to resolve whether mutant transcripts were absent from any fraction or whether they were undetectable by Northern analysis due to their heterogeneous nature. We therefore performed real-time RT-PCR on chromatin and nucleoplasmic RNA isolated from HeLa cells transfected with each β-globin plasmid as well as the VA control plasmid. cDNA was synthesised using random hexamers together with a primer specific to β-globin exon 3 and exon 3 containing RNA was quantitated by real-time PCR (Figure 1E). This assay permits detection of the total population of RNA containing exon 3 even if it is heterogeneous in nature. Differences in transfection and fractionation efficiencies were corrected for by analysing VA and GAPDH RNA levels (see Materials and methods). Interestingly, there were similar levels of exon 3 RNA in all chromatin samples. These data imply that product deriving from mutant chromatin RNA cannot be detected by Northern Analysis due to its heterogeneous nature. Consistent with the Northern analysis, we detected high levels of exon 3 containing WT RNA in the nucleoplasm, indicating efficient release of these RNAs. In contrast, only half as much In1m RNA was recovered from the nucleoplasm compared to chromatin and even less was detected in pAm, ΔTIn1m and ΔTpAm nucleoplasmic samples. Thus, mutant nucleoplasmic RNA is detected at much lower amounts than WT RNA by both Northern and qRT-PCR analysis. We conclude that mutated β-globin RNA is predominantly chromatin-based, which is consistent with previous reports utilising microscopy-based approaches (Custodio *et al*, 1999). The release of more In1m transcripts compared to the other mutant RNAs might be explained by observations that Pol II termination is occurring on this construct (Supplementary Figure 1 and (Dye and Proudfoot, 1999)). In line with this, Pol II termination is important for the release of RNA from chromatin (West *et al*, 2008).

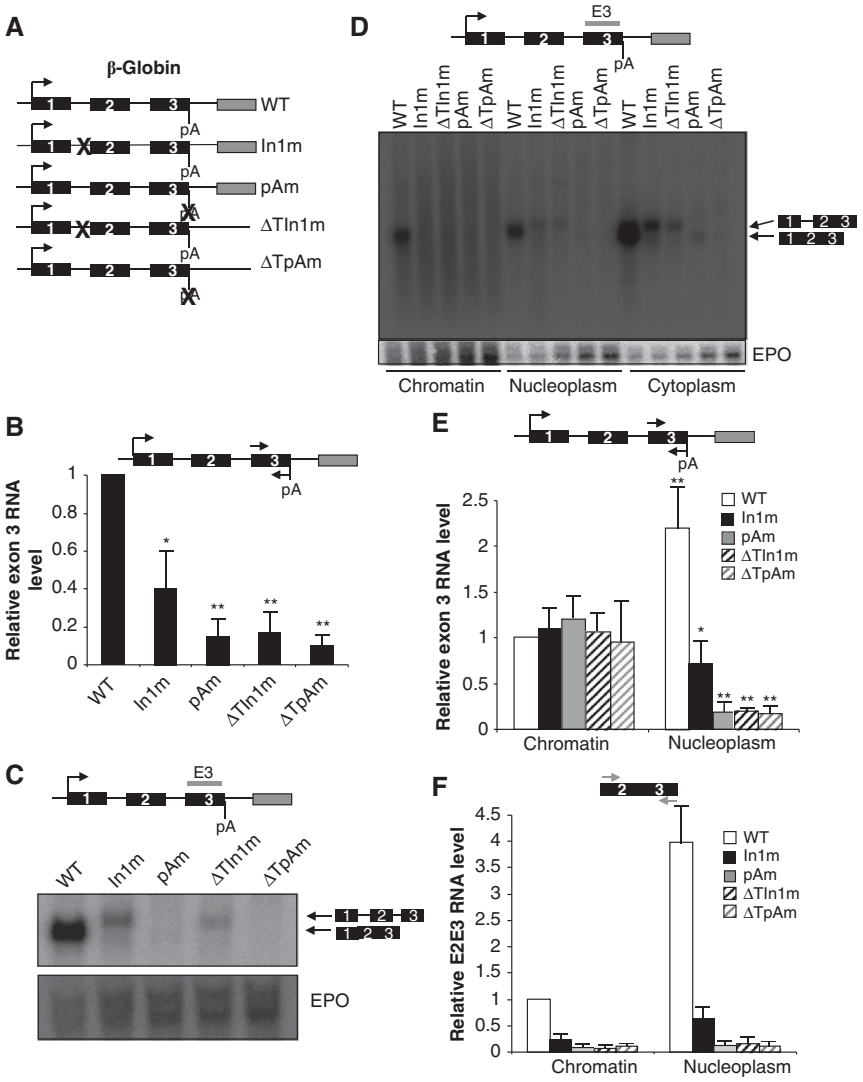

Figure 1 Aberrant β-globin transcripts are degraded at chromatin sites. **(A)** Schematic diagram of the plasmids used to study β-globin pre-mRNA degradation. The HIV promoter (arrow) is followed by the β-globin gene with numbered exons (black boxes), pA signal (pA), and terminator element (grey box) indicated. The In1m, pAm, ΔTIn1m and ΔTpAm derivatives are also shown and the position of respective mutations is indicated with a cross. **(B)** Real-time PCR analysis of exon 3-containing β-globin transcripts in total RNA isolated from WT, In1m, pAm, ΔTIn1m and ΔTpAm transfected cells. Diagram shows the position of the primer pair (arrows). Quantitation is expressed in relation to values obtained from WT samples, which were set to 1 following normalisation to signal from co-transfected VA. **(C)** Northern blotting of total RNA isolated from WT, In1m, pAm, ΔTIn1m and ΔTpAm transfected cells. Spliced and partially spliced products as well as the EPO co-transfection product are indicated. Diagram shows exon 3 probe (grey line). **(D)** Northern blotting of chromatin-associated, nucleoplasmic and cytoplasmic RNA isolated from WT, In1m, pAm, ΔTIn1m and ΔTpAm transfected cells. Spliced and partially spliced products as well as the EPO co-transfection product are indicated. Diagram shows exon 3 probe (grey line). **(E)** Real-time PCR analysis of exon 3 β-globin transcript levels in chromatin-associated and nucleoplasmic RNA isolated from cells transfected with WT, In1m, pAm, ΔTIn1m or ΔTpAm. Diagram shows the positions of primer pairs used. Quantitation is in relation to values obtained from WT samples, which were set to 1 following normalisation to signal from co-transfected VA. **(F)** Real-time PCR analysis of exon 2-exon 3 β-globin transcript levels in chromatin-associated and nucleoplasmic RNA isolated from cells transfected with WT, In1m, pAm, ΔTIn1m or ΔTpAm. Diagram shows the positions of primer pairs used. Quantitation is in relation to values obtained from WT samples, which were set to 1 following normalisation to signal from co-transfected VA. All error bars represent the standard deviation from the mean (s.d.) from a minimum of three biological replicates. * and **indicate *P*-values of <0.05 and <0.01 respectively. Figure source data can be found with the Supplementary data.

We next analysed spliced (exon 2-exon 3) RNA from the same samples (Figure 1F). As with exon 3 RNA, spliced WT transcript were efficiently released into the nucleoplasm. There were much fewer spliced transcripts in the chromatin fraction for all mutant transcripts compared to WT, which is consistent with the above Northern analysis and reflects the expected impairment of splicing caused by the mutations. Similarly, very little spliced mutant transcripts were observed in the nucleoplasm. We also analysed the location of exon 1-exon 2 products in WT, pAm and ΔTpAm (Supplementary Figure 2). Although similar levels of this product were observed between the WT and mutant transcripts in the chromatin fraction only WT RNA was released into the nucleoplasm. Thus, a single successful splicing event is insufficient for release. In summary, although similar levels of chromatin RNA are recovered from WT and mutant gene templates, WT transcripts are much more efficiently processed and released as judged by their recovery in the

nucleoplasmic and cytoplasmic fractions. The presence of lower overall levels of mutant RNAs implies that they are degraded, which is likely to be a result of impaired processing. Since we only recover large amounts of mutant RNA from the chromatin fraction, we hypothesised that degradation was most likely to occur at the chromatin or otherwise very soon after release into the nucleoplasm.

The role of exonucleases in degrading aberrant β-globin transcripts

We sought to identify the enzymes responsible for nuclear degradation of the mutant β-globin transcripts and to determine whether degradation was associated with the chromatin or nucleoplasmic fractions. We initially analysed the human homologue of *S. cerevisiae* Rrp6 (hRrp6), since previous reports indicated an important function for it in human pre-mRNA surveillance (de Almeida *et al*, 2010; Eberle *et al*, 2010). We used RNAi to deplete hRrp6 from HeLa cells (Figure 2A). Chromatin-associated and nucleoplasmic RNA was isolated from mock treated and hRrp6 depleted cells transfected with each β-globin construct and the VA plasmid. Following reverse transcription, cDNA was amplified with primers directed to exon 3 (Figure 2B). After normalising to VA, similar levels of WT RNA were observed in mock treated and hRrp6 depleted cells indicating that these transcripts are not substrates for this protein. There were modest increases in mutant transcripts levels in the chromatin and nucleoplasmic fractions upon hRrp6 depletion, which we also observed upon depleting the Rrp44/Dis3 subunit of the exosome (Supplementary Figure 3). Although these effects are small, they are consistent with previous reports of hRrp6 function in the surveillance of aberrant β-globin RNAs (de Almeida *et al*, 2010; Eberle *et al*, 2010).

The small effects observed following depletion of catalytic exosome components may reflect the activity of residual protein remaining following siRNA treatment or the compensatory action of the other catalytic subunit. There may also be other transcript degradation pathways operating on the RNAs studied here. Indeed, many budding yeast pre-mRNAs are sensitive to depletion of either the exosome or the $5'\rightarrow3'$ exonuclease, Rat1 (Bousquet-Antonelli *et al*, 2000; Egecioglu *et al*, 2011). To study any role for the human homologue of Rat1, Xrn2, we depleted it from HeLa cells using RNAi (Figure 2C). Chromatin-associated and nucleoplasmic RNA was then isolated from mock treated and Xrn2 depleted cells transfected with the β-globin plasmids and the VA plasmid. Following reverse transcription with an exon 3 specific primer, cDNA was analysed by real-time PCR using exon 3 primers (Figure 2D). Depletion of Xrn2 did not alter the level of WT transcripts in either nuclear fraction after normalising to VA. In1m transcripts were also unaffected indicating that they are also not substrates for Xrn2. However, pAm, ΔTIn1m and ΔTpAm transcripts were stabilised in both fractions upon Xrn2 depletion. It is interesting that Xrn2 does not target In1m transcripts but degrades ΔTIn1m RNAs. This differential effect might be explained by the efficient termination on In1m (Supplementary Figure 1 and (Dye and Proudfoot, 1999)), which might facilitate the escape of transcripts from chromatin associated Xrn2. Importantly, Xrn2 depletion stabilised chromatin and nucleoplasmic transcripts to an equal degree (~2–3-fold). Because most of these mutant RNAs are chromatin-associated (Figure 1E), this strongly suggests that the majority of Xrn2 sensitive transcripts are also chromatin-associated. If degradation was nucleoplasmic, we would instead expect a larger effect in this fraction with minimal stabilisation of chromatin RNA.

We also analysed the effect of Xrn2 depletion on the level of spliced β-globin transcripts (exon2-exon3) from each gene version in chromatin and nucleoplasmic fractions (Figure 2E). There was no effect of Xrn2 depletion on spliced WT or In1m transcripts. However, Xrn2 depletion increased the level of spliced transcripts for all other mutant β-globin versions and in each cell fraction. This suggests that spliced mutant transcripts are also substrates for Xrn2 or that reduced degradation allows a suboptimal splicing process to succeed.

Degradation by Xrn2 is co-transcriptional

We wished to explore the potential function for Xrn2 in degrading aberrant transcripts further given that its role in human nuclear RNA turnover is less well characterised than that of the exosome. In particular, the stabilisation of chromatin-associated RNA upon its depletion indicates a co-transcriptional degradation process given previous findings that this fraction is enriched in nascent RNA (Wuarin and Schibler, 1994). To test this hypothesis, we developed an alternative means to isolate a purer nascent RNA fraction. We performed a nuclear run on (NRO) assay to label nascent RNA with 4-thioUTP (Figure 3A). During NRO, Pol II elongates 100–200 nucleotides thereby labelling the very 3′ end of nascent RNA (Dye and Proudfoot, 2001; Core *et al*, 2008). 4-thio UTP labelled nascent RNA is then biotinylated and specifically enriched from non-labelled RNA following capture by streptavidin coated beads. NRO RNA is normally fragmented to resolve positions of actively transcribing Pol II but we left the transcripts intact to better determine their splicing status and stability.

It was important to initially test whether the assay was capable of detecting Xrn2-dependent changes in nascent RNA levels. We showed that this was the case by detecting the increased levels of read-through β-globin transcripts previously shown, by NRO, to accumulate following Xrn2 depletion (Supplementary Figure 4) and (West *et al*, 2004). Next, we performed this procedure on nuclei isolated from mock or Xrn2 depleted HeLa cells transfected with WT, ΔTIn1m or ΔTpAm, together with VA (Figure 3B). Isolated nascent transcripts were reverse transcribed and subjected to real-time PCR analysis to quantitate both exon 3 containing and spliced (exon 2-exon 3) RNA. After normalising to VA, no change in the level of WT transcripts was observed between the control and Xrn2 depleted cells consistent with the Figures 2D and E. However, ~2-fold more nascent exon 3 containing and spliced RNA was observed in Xrn2 depleted cells transfected with ΔTIn1m or ΔTpAm. These data provide additional evidence that many ΔTIn1m and ΔTpAm transcripts are co-transcriptionally degraded by Xrn2.

Pol II loading is unchanged by Xrn2 depletion

An alternative explanation for increased levels of aberrant pre-mRNA in Xrn2 depleted cells would be increased Pol II density on mutant gene templates leading to greater RNA production. We tested for this by analysing Pol II loading by chromatin immunoprecipiation (ChIP). Antibodies to total/serine 5 phosphorylated CTD (4H8) or to serine 2 phosphory-

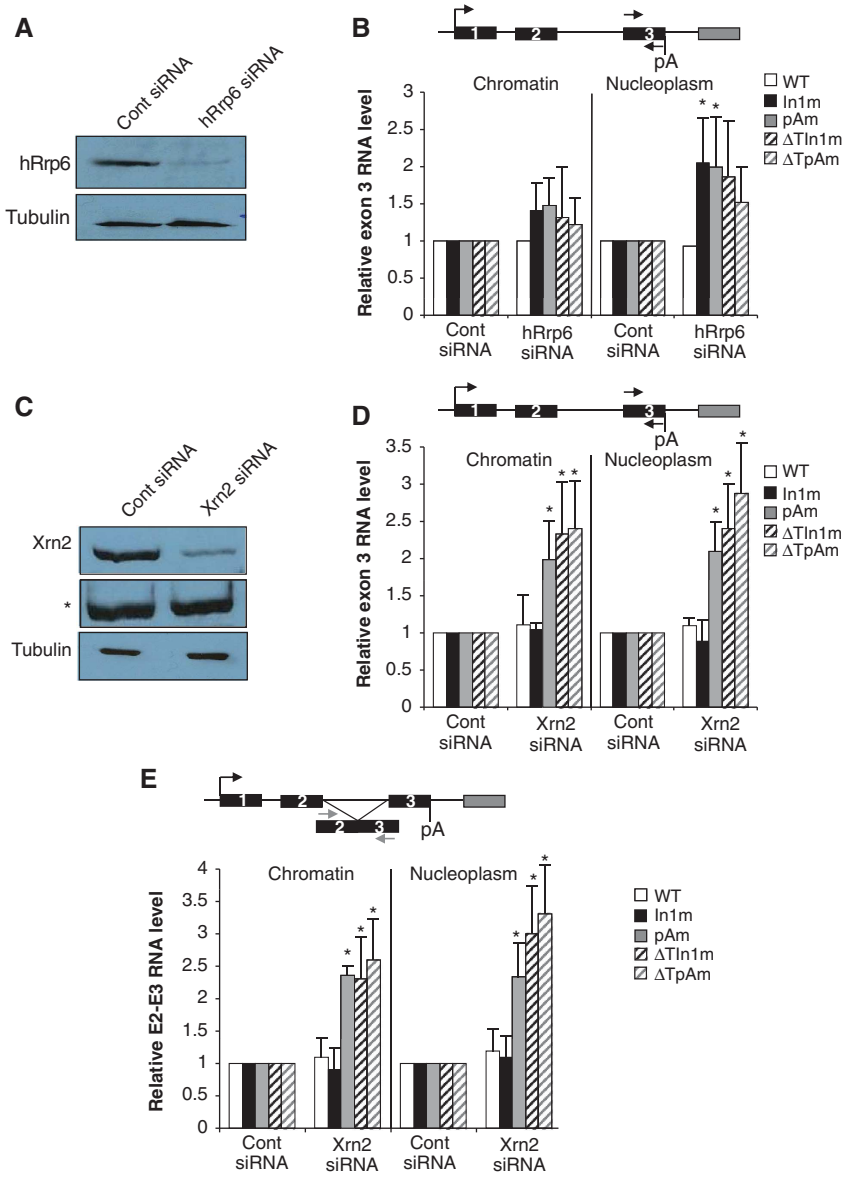

Figure 2 Roles of hRrp6 and Xrn2 in the degradation of aberrant β-globin transcripts. **(A)** Western blot showing RNAi depletion of hRrp6 protein. Antibodies were used to detect γ-Tubulin (lower panel) or hRrp6 (top panel) in extracts from cells transfected with control or hRrp6-specific siRNA. **(B)** Real-time PCR analysis of exon 3-containing β-globin transcripts in chromatin-associated and nucleoplasmic RNA samples obtained from mock or hRrp6 depleted cells transfected with WT, In1m, pAm, ΔTIn1m or ΔTpAm. The diagram shows the position of primers (arrows). For each transfected gene, values obtained from mock treated cells were set to 1 following normalisation to signal from co-transfected VA. **(C).** Western blot showing RNAi depletion of Xrn2 protein. Antibodies were used to detect γ-Tubulin (lower panel) or Xrn2 (top panel) in extracts from cells transfected with control or Xrn2-specific siRNA. Middle panel (marked *) shows a non-specific band detected by the Xrn2 antibody, which acts as an additional loading control. **(D)** Real-time PCR analysis of exon 3-containing β-globin transcripts in chromatin-associated and nucleoplasmic samples obtained from mock or Xrn2 depleted cells transfected with WT, In1m, pAm, ΔTIn1m or ΔTpAm. The diagram shows the position of primers (black arrows). For each transfected gene, values obtained from mock treated cells were set to 1 following normalisation to signal from co-transfected VA. **(E)** Real-time PCR analysis of spliced (exon2-exon3) β-globin transcripts in chromatin-associated and nucleoplasmic samples obtained from mock or Xrn2 depleted cells transfected with WT, In1m, pAm, ΔTIn1m or ΔTpAm. Diagram shows position of primers (grey arrows). For each transfected gene, values obtained from mock treated cells were set to 1 following normalisation to signal from co-transfected VA. All error bars represent the s.d. from a minimum of three biological replicates. *indicates *P*-value of <0.05. Figure source data can be found with the Supplementary data.

lated CTD (S2) were used to immunoprecipitate DNA from control or Xrn2 depleted cells transfected with ΔTIn1m and ΔTpAm (Figure 3C). Although ChIP on plasmid DNA is notoriously difficult to perform, we obtained significant above-background signal following extensive washing and the use of dynabeads rather than agarose beads (see Materials and methods). We analysed regions over exons 1 and 3 on both plasmids but observed no evidence of higher Pol II loading in response to Xrn2 depletion. ChIP using an antibody (8WG16) to unphosphorylated CTD also revealed no effect of Xrn2 depletion (our unpublished data). It therefore seems likely that the elevated RNA levels observed following Xrn2 depletion result from reduced degradation rather than increased Pol II occupancy.

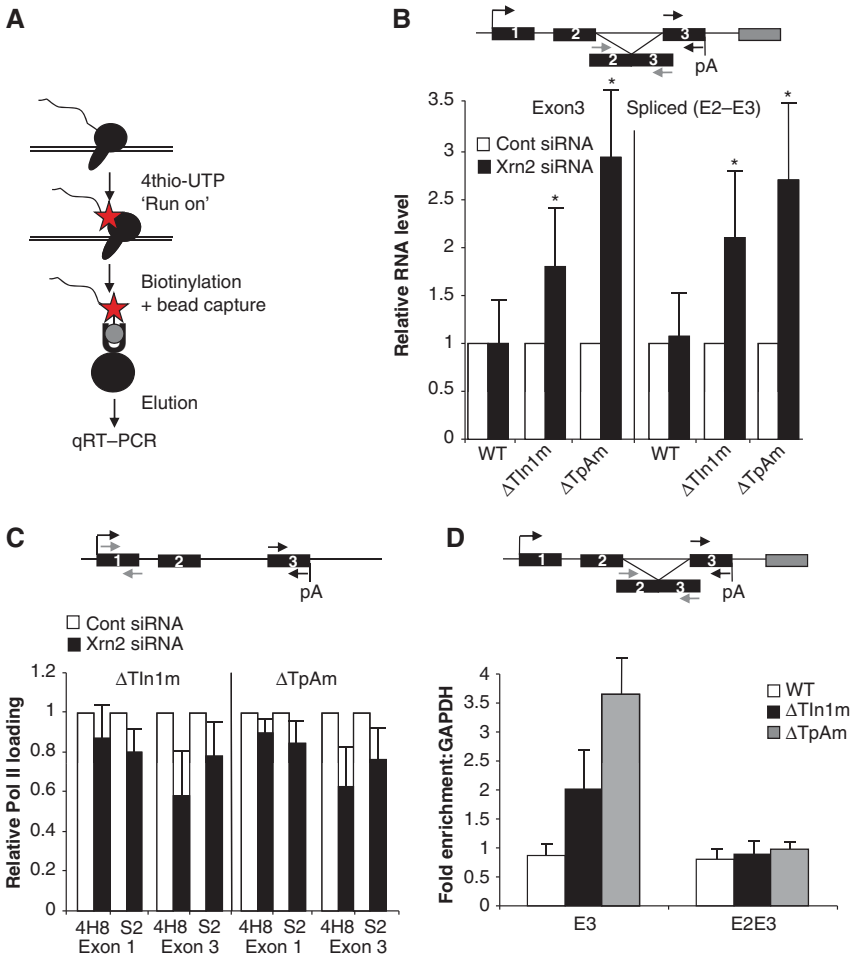

Figure 3 Actively transcribed nascent RNAs are bound to and degraded by Xrn2. **(A)** Diagram of 4-thio UTP NRO procedure. Pol II in isolated nuclei was 'run on' in the presence of 4thio UTP (star). Nascent, 4-thio UTP labelled, transcripts were purified by biotinylation (grey circle) and selection with streptavidin magnetic beads (black circle). These were then analysed by reverse transcription and real-time PCR. **(B)** Real-time PCR analysis of exon3-containing and spliced β-globin transcripts in nascent RNA samples obtained from mock or Xrn2 depleted cells transfected with WT, ΔTIn1m or ΔTpAm. Samples obtained from Xrn2 depleted cells were quantitated in relation to those obtained from control samples, which were set at 1 following normalisation to signal from co-transfected VA. **(C)** Analysis of Pol II loading on ΔTIn1m or ΔTpAm plasmids in mock and Xrn2 depleted cells using ChIP. Diagram shows positions of the PCR amplicons to detect Pol II loading at the promoter (grey arrows) and exon 3 (black arrows). Graph shows relative Pol II loading, calculated from the % input of each immunoprecipitation, which was given a value of 1 in control cells. **(D)** RNA immunoprecipitation analysis of Xrn2 bound transcripts in WT, ΔTIn1m and ΔTpAm transfected cells. Diagram shows positions of PCR amplicons to detect exon 3 (black arrows) and spliced (grey arrows) transcripts. Quantitation is expressed as fold enrichment over background expressed relative to that found for GAPDH mRNA, which was given a value of 1. All error bars represent the s.d. from a minimum of three biological replicates. *indicates *P*-value of <0.05.

Mutant transcripts are bound by Xrn2 in vivo

To get more direct evidence that Xrn2 degrades some mutant transcripts, we wanted to test whether Xrn2 binds mutant transcripts *in vivo*. RNA from cross-linked extracts isolated from HeLa cells transfected with WT, ΔTIn1m or ΔTpAm was immunoprecipitated with Xrn2-specific antibodies. cDNA was subsequently synthesised with random hexamers and the β-globin exon 3 reverse primer. We then analysed exon 3 and spliced (exon 2-exon 3) β-globin as well as spliced GAPDH transcripts in all samples by real-time PCR (Figure 3D). Results were expressed as fold enrichment over background (no antibody control). All results were shown relative to the enrichment observed for GAPDH mRNA, which we used as a negative control. We did not observe any enrichment of exon 3 or spliced RNA in WT samples consistent with it not being an Xrn2 substrate. However, in ΔTIn1m and particularly in ΔTpAm samples, we observed significant enrichment of exon 3 RNA. Since exon 3 RNA is predominantly unprocessed and chromatin associated in the mutant samples (Figure 1 and Supplementary Figure 1), these data indicate that nascent transcripts that fail to be processed are bound by Xrn2 *in vivo*. Interestingly spliced mutant transcripts were not bound suggesting that splicing prevents degradation by Xrn2.

Co-transcriptional degradation of aberrant endogenous pre-mRNA

Our data provide strong evidence for co-transcriptional degradation of some aberrant β-globin transcripts by Xrn2. However, plasmid transcription may not necessarily reflect chromosomal transcription and most human genes are longer and more complex than β-globin. We therefore wished to examine whether co-transcriptional degradation of aberrant pre-mRNA is a process relevant to endogenous genes. To our knowledge, nuclear degradation of longer human pre-mRNAs

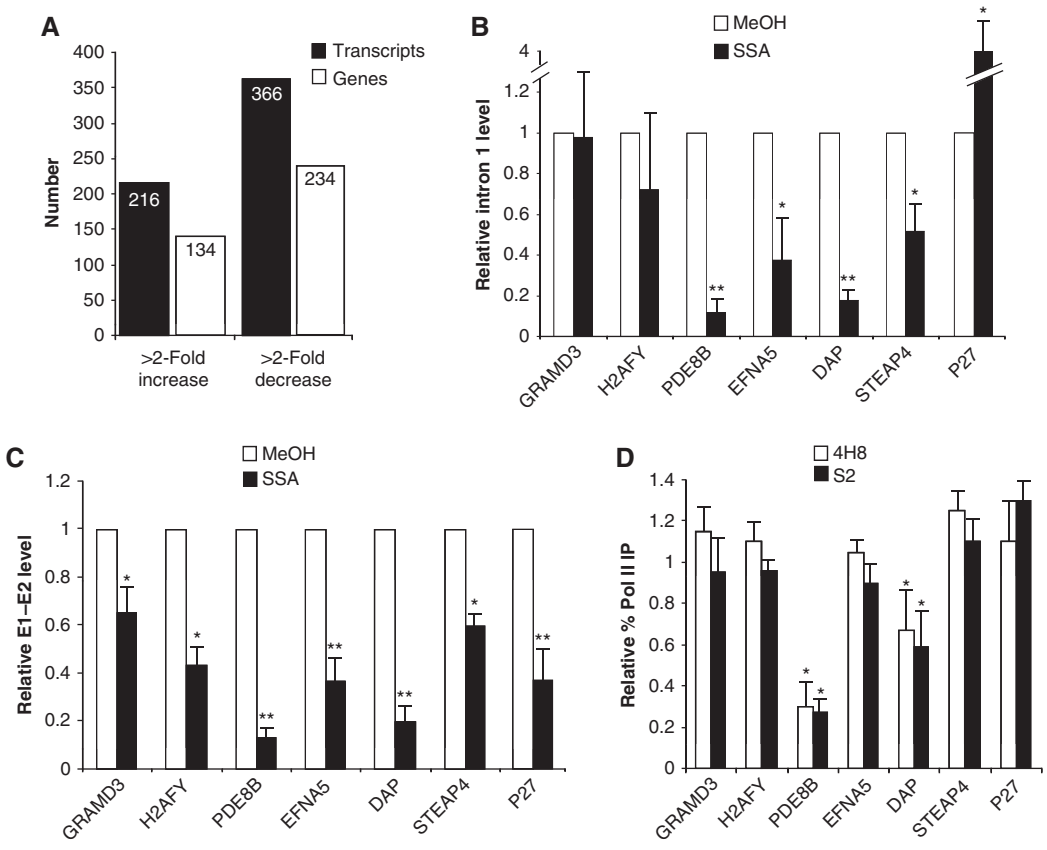

Figure 4 Co-transcriptional degradation of endogenous pre-mRNAs following Spliceostatin A treatment. **(A)** Bioinformatic analysis of transcripts and genes containing introns that are either increased or decreased by 2-fold or more upon SSA treatment. **(B)** Real-time PCR analysis of intron transcripts in chromatin-associated RNA isolated from control (MeOH) or SSA treated cells. Primer pairs detected the first intron from GRAMD3, H2AFY, PDE8B, EFNA5, DAP, STEAP4 or P27 transcripts. Graph shows quantitation where the value obtained from control cells were set to 1 following adjustment to TAF7 levels. **(C)** Real time PCR analysis of spliced transcripts is chromatin-associated RNA isolated from control (MeOH) or SSA treated cells. Primer pairs detected spliced transcripts (exon1-exon2) from GRAMD3, H2AFY, PDE8B, EFNA5, DAP, STEAP4 or P27 genes. Graph shows quantitation where the value obtained from control cells were set to 1 following adjustment to TAF7 levels. **(D)** Analysis of Pol II loading on GRAMD3, H2AFY, PDE8B, EFNA5, DAP, STEAP4 or P27 genes in control (MeOH) and SSA treated cells using ChIP. The %IP of input was calculated for each probe in each sample. %IP of each amplicon is shown for SSA treated cells but was compared to that obtained in control cells, where the value was set to 1. All error bars represent the s.d. from a minimum of three biological replicates. * and **indicate *P*-value of <0.05 and <0.01 respectively.

produced from their natural chromosomal position has not been investigated. To do so, we generated a pool of aberrant pre-mRNA transcripts by treating cells with Spliceostatin A (SSA) (Kaida *et al*, 2007). SSA prevents proper function of SF3b, frequently resulting in a block at the first step of splicing and often leading to aberrant alternative splicing (Kaida *et al*, 2007; Roybal and Jurica, 2010; Corrionero *et al*, 2011). We reasoned that SSA treatment should generate some transcripts that are substrates for Xrn2 if the protein plays a more widespread role in the turnover of aberrant pre-mRNA.

A recent microarray analysis looked at the effects of SSA on pre-mRNA transcripts from human chromosomes 5, 7 and 16 (Kaida *et al*, 2010). 216 transcripts showed evidence of intron accumulation, which would be one expected consequence of splicing inhibition. However, inefficient splicing might promote transcript degradation and reduce pre-mRNA levels. We analysed the data from Kaida *et al* for evidence of transcripts that are reduced by 2 or more fold following SSA treatment. Using the same search criteria, we found 366 such transcripts (Figure 4A). Since some of these transcripts originate from the same gene we also used Ensembl 61 gene models to analyse the data and find the number of genes whose transcripts are affected. We found 134 and 234 genes whose transcripts were, respectively, 2-fold or more up or down regulated following SSA treatment. Whilst reduced transcription is a possible explanation for lower levels of RNA, it is also possible that degradation is responsible in some cases.

We selected six transcripts that showed a range in fold change of intron reduction in the microarray analysis following SSA treatment: GRAMD3, H2AFY, PDE8B, DAP, EFNA5 and STEAP4. Unlike β-globin, each of these genes is long and contains multiple introns. To check the effect of SSA on nascent RNA from these genes, chromatin RNA was isolated from SSA or MeOH (control) treated cells and reverse transcribed with random hexamers. cDNA was then real-time PCR amplified to detect intron 1 containing species (Figure 4B). As additional controls, we analysed TAF7 and P27 transcripts. TAF7 is intronless and controls for non-specific SSA effects whereas P27 transcripts are known to accumulate following SSA treatment (Kaida *et al*, 2007). After normalising to TAF7 levels, we observed a ~4-fold increase in P27 pre-mRNA levels, which confirms previous results and

demonstrates the inhibitory effect of SSA on co-transcriptional splicing in our system. In contrast, no accumulation of intronic RNA was evident on any of the other transcripts analysed. GRAMD3 and H2AFY levels were similar in control and SSA treated cells whereas DAP, PDE8B, EFNA5 and STEAP4 levels were reduced. It has been shown that several transcripts, including P27, accumulate in nucleoplasmic foci following SSA treatment (Kaida *et al*, 2007; Brody *et al*, 2011; Martins *et al*, 2011). Consistent with this result we also noted a strong accumulation of P27 pre-mRNA in the nucleoplasm following SSA treatment; however the other six transcripts remained predominantly chromatin-associated (Supplementary Figure 5). These data highlight distinct effects of SSA on P27 pre-mRNA levels and location as compared to the other six transcripts analysed.

We next analysed the effect of SSA on co-transcriptional splicing of the transcripts analysed above. cDNA generated from chromatin-associated RNA isolated from control and SSA treated cells was real-time PCR amplified using primers to detect exon 1-exon 2 splicing (Figure 4C). As expected, a ~3-fold reduction in splicing was observed for P27. Reductions were also observed for the other six transcripts with splicing least affected for the GRAMD3 gene. In the absence of any degradation, a reduction in spliced transcripts might lead to a corresponding increase in unspliced RNA and this is observed for P27 (compare Figure 4B and C). Such an increase in intron levels was not evident for the other six transcripts, which might be due to their degradation.

A reduction in transcript levels in response to SSA could be also explained by reduced Pol II occupancy on these genes. Indeed, mutant β-globin genes, when stably integrated into chromosomes, sometimes support lower Pol II occupancy (de Almeida *et al*, 2010; Mapendano *et al*, 2010; Martins *et al*, 2011). We tested for this in our system by analysing Pol II loading over the same amplicons used for real-time PCR analysis using ChIP with the 4H8 and S2 antibodies in control and SSA treated cells (Figure 4D). In most cases, we observed little difference in Pol II loading. There was a significant reduction on the PDE8B and DAP genes upon SSA treatment but this was less marked than the reduction in RNA observed. Therefore, while reduced transcription upon SSA treatment occurs in some cases, it may not fully explain the reduction in RNA levels observed in Figure 4B. Collectively, these data suggest that degradation may account for some pre-mRNA loss following SSA treatment.

Xrn2 degrades pre-mRNAs following SSA treatment

We therefore tested whether Xrn2 is involved in the co-transcriptional degradation of the above six transcripts following SSA treatment. Mock treated and Xrn2 depleted cells were treated with MeOH or SSA before isolation of chromatin-associated RNA. The four RNA samples were then subjected to real-time PCR analysis to quantitate the same intron 1 transcripts from each gene (Figure 5A). After correction to TAF7 levels, there was little difference in the level of any transcript between MeOH treated mock and Xrn2 depleted cells suggesting that Xrn2 does not degrade these transcripts under normal conditions. Following SSA treatment, we also observed little effect of Xrn2 depletion on P27 transcripts. Interestingly P27 transcripts are released into the nucleoplasm following SSA treatment (Supplementary Figure 5). As with β-globin In1m transcripts (Figure 2D),

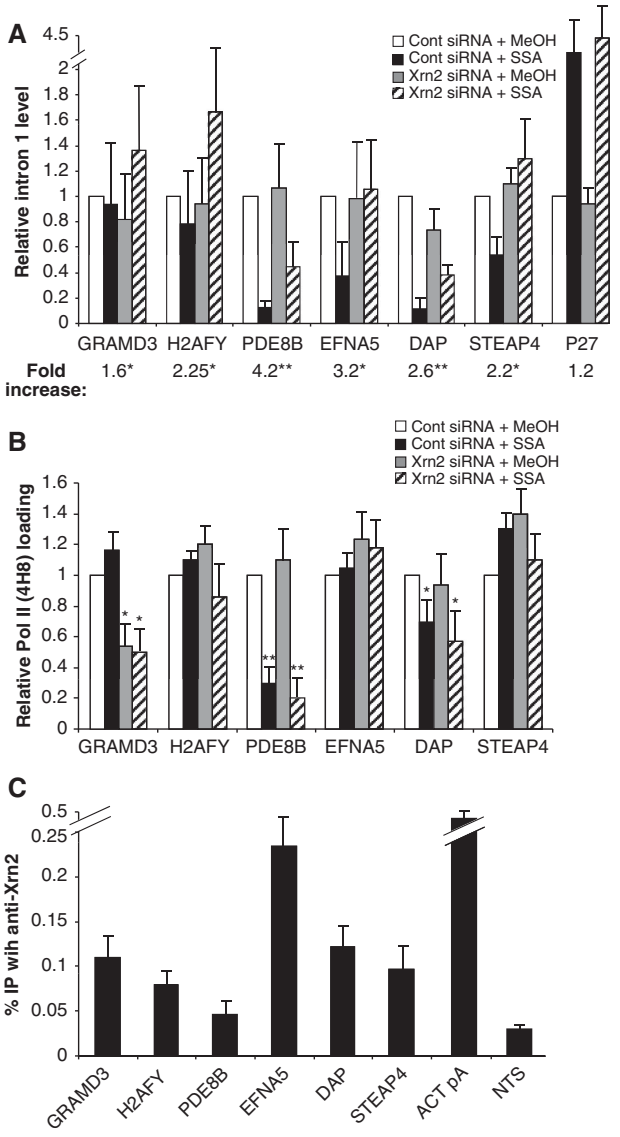

Figure 5 Xrn2 degrades endogenous pre-mRNAs following treatment with Spliceostatin A. **(A)** Real-time PCR analysis of intron transcripts in chromatin-associated RNA isolated from mock treated or Xrn2 depleted cells treated with MeOH or SSA. Primer pairs detected the first intron from GRAMD3, H2AFY, PDE8B, EFNA5, DAP, STEAP4 or P27 transcripts. Graph shows quantitation where the values obtained from control siRNA transfected cells treated with MeOH were given a value of 1 after adjustment to TAF7 levels. Fold increase was calculated from the product ratio in SSA:MeOH in control and Xrn2 depleted cells and was given a value of 1 in control cells. **(B)** ChIP analysis of Pol II loading (4H8 antibody) in mock treated or Xrn2 depleted cells treated or not with SSA. Graph shows relative Pol II loading, calculated from the % input of each immunoprecipitation, which was given a value of 1 in control siRNA transfected cells treated with MeOH. **(C)** ChIP of Xrn2 recruitment to chromatin. Quantitation is expressed as percentage of input DNA immunoprecipitated with anti-Xrn2. The NTS signal derives from a region on chromosome 10 with no annotated genes. All error bars represent the s.d. from a minimum of three biological replicates. * and **indicate *P*-values of <0.05 and <0.01 respectively.

this may facilitate their evasion of Xrn2 activity at the transcription site (see discussion). Importantly, we observed an SSA-dependent increase in the level of all other transcripts upon Xrn2 depletion. Similar differences were also observed

when we used alternative primer pairs in different positions on the same transcripts (Supplementary Figure 6). Interestingly, hRrp6 depletion had no substantial effect on any of the transcripts studied implying that it is not necessary for their degradation and perhaps indicating redundancy between the exosome and Xrn2 (Supplementary Figure 7). We also found no evidence that nonsense-mediated decay is involved in degrading any of the six transcripts affected by Xrn2 (Supplementary Figure 8). These data implicate Xrn2 in the degradation of many aberrant pre-mRNAs induced by SSA treatment.

We next wanted to rule out the possibility of increased Pol II loading upon Xrn2 depletion combined with SSA accounting for increased RNA levels. We therefore performed Pol II ChIP on control and Xrn2 depleted cells with or without SSA using the 4H8 antibody and the same intron 1 amplicons (Figure 5B). With the exception of GRAMD3, where a reduction in Pol II loading was observed in Xrn2 depleted cells, there was no change in Pol II ChIP signal as a result of Xrn2 depletion. In addition, no large changes in Pol II loading were seen in Xrn2 depleted and SSA treated cells when compared to control cells treated with SSA. Similar results were achieved with the S2 antibody (Supplementary Figure 9).

Xrn2 is present over relevant regions

Co-transcriptional degradation of pre-mRNA transcripts by Xrn2 would require the protein to operate in regions of the gene upstream from the poly(A) site. Consistent with this possibility, Rat1 and Xrn2 are detectable by ChIP over such regions (Kaneko *et al*, 2007; Kim *et al*, 2010). We therefore wished to determine whether Xrn2 associated with regions from which its substrates were generated (Figure 5C). We performed ChIP analysis using an Xrn2-specific antibody since the RIP technique employed in Figure 3D was not sensitive enough to detect the low level transcripts produced in this experiment. As a positive control we assayed DNA around the actin poly(A) site, which was previously shown to be immunoprecipitated with this Xrn2 antibody (Kaneko *et al*, 2007). As expected, we were able to immunoprecipitate this DNA with the Xrn2 antibody. As a negative control, we analysed a part of chromosome 10 used by others as a non-transcribed control region (Listerman *et al*, 2006). Very little of this DNA was immunoprecipitated. Importantly, we observed significant immunoprecipitation of the regions from which Xrn2 sensitive transcripts were produced following SSA treatment. A similar result was obtained using an additional Xrn2 antibody (Supplementary Figure 10). This suggests that Xrn2 is located in close proximity to regions where aberrant transcripts arise.

Dcp2 depletion stabilises some transcripts following SSA treatment

Unregulated degradation of RNA from the 5′ end is normally prevented by the cap, which is resistant to Xrn2 degradation (Stevens and Maupin, 1987). Thus a decapped terminus must be generated prior to degradation by Xrn2 and this could be achieved by decapping or endonucleolytic cleavage. Dcp2 is a major decapping activity conserved in all eukaryotes. The majority of human Dcp2, when tagged with fluorescent protein, localizes to the cytoplasm (van Dijk *et al*, 2002). However, imaging of endogenous Dcp2 revealed a nuclear population of the protein that could be relevant to the current

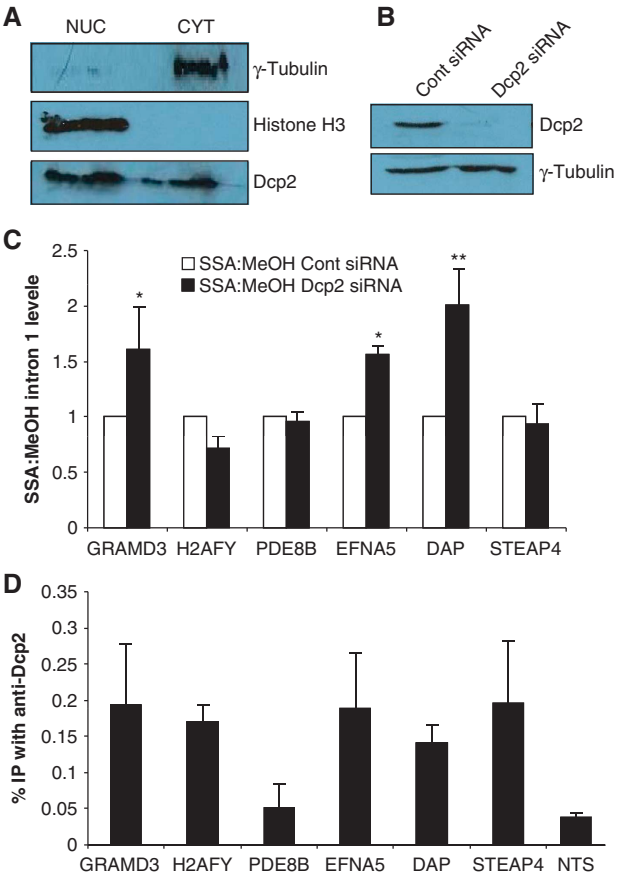

Figure 6 Dcp2 depletion stabilises some SSA sensitive transcripts. **(A)** Western blotting of nuclear and cytoplasmic protein fractions analysing γ-Tubulin (top panel), Histone H3 (middle panel) and Dcp2 (lower panel). **(B)** Western blot showing RNAi depletion of Dcp2 protein. Antibodies were used to detect γ-Tubulin (lower panel) or Dcp2 (top panel) in extracts from cells transfected with control or Dcp2-specific siRNA. **(C)** Real-time PCR analysis of intron transcripts in chromatin-associated RNA isolated from mock treated or Dcp2 depleted cells treated with MeOH or SSA. Primer pairs detected the first intron from GRAMD3, H2AFY, PDE8B, EFNA5, DAP or STEAP4 transcripts. Graph shows quantitation, which is presented as a ratio of each product in SSA vs MeOH treated cells. The value for each primer pair obtained in mock siRNA treated cells was set to 1. **(D)** ChIP of Dcp2 recruitment to chromatin. Quantitation is expressed as percentage of input DNA immunoprecipitated with anti-Dcp2. The NTS signal derives from a region on chromosome 10 with no annotated genes. All error bars represent the s.d. from a minimum of three biological replicates. * and **indicate *P*-values of <0.05 and <0.01 respectively. Figure source data can be found with the Supplementary data.

study (Liu *et al*, 2004). To analyse the location of Dcp2 in HeLa cells, we performed western blotting on nuclear and cytoplasmic protein fractions (Figure 6A). The efficiency of the fractionation procedure was verified by analysis of Histone H3 and γ-Tubulin, which were predominantly nuclear and cytoplasmic respectively. Dcp2, however, was found in both fractions indicating that there is a nuclear population of the protein. This remained the case after additional washing of the nuclei prior to blotting (Supplementary Figure 11). To test whether Dcp2 might be required to degrade aberrant transcripts following SSA treatment, we used RNAi to deplete it from HeLa cells the success of which was confirmed by western blotting (Figure 6B). Next, total RNA was isolated from control and Dcp2 depleted cells treated or not with SSA.

Following cDNA synthesis with random hexamers, real-time PCR was performed to detect intron 1 containing transcripts from the six genes under study (Figure 6C). Three transcripts (DAP, EFNA5 and GRAMD3) were modestly stabilised in SSA treated Dcp2 depleted cells when compared to SSA treated control cells. These data suggest that decapping by Dcp2 can often generate an entry site for Xrn2 to degrade aberrant RNA.

Finally, we tested whether Dcp2 was present on transcribed genes using ChIP (Figure 6D). Consistent with a potential for decapping of aberrant pre-mRNA, we found Dcp2 to be present on most of our tested genes (Supplementary Figure 11). Only a slightly above-background signal was observed on PDE8B, which may reflect a lack of Dcp2 recruitment to that region or the low transcriptional activity on that gene. Similar results, though with lower immunoprecipitation, were obtained with a separate Dcp2 antibody (Supplementary Figure 11). Overall these data implicate Dcp2 in the degradation of some but not all pre-mRNAs following SSA addition. Since many aberrant transcripts are not stabilised by Dcp2 depletion, it seems likely that there are other means of generating decapped substrates for Xrn2 to degrade (see discussion).

Discussion

One of the major conceptual advances in the transcription and pre-mRNA maturation fields has been the discovery that the two processes are functionally coupled (McCracken *et al*, 1997). As a consequence, it is now known that most splicing and 3′ end processing occur co-transcriptionally *in vivo*. Since aberrantly retained introns or uncleaved poly(A) sites would normally have been processed during transcription it is logical to propose that such species are degraded co-transcriptionally. This is an efficient way to remove potentially harmful transcripts and prevents the synthesis of unproductive transcripts.

Once a transcript has been identified as defective, the appropriate degradation machinery must be activated or recruited to elicit transcript decay. This could be achieved by recruitment of degradation factors. However, our ChIP data show that both Xrn2 and Dcp2 are present on genes even under conditions where splicing is not inhibited. These data strongly suggest that these factors are always associated with transcription but only become active in the event of defective RNA biogenesis. Given that our data are consistent with degradation being co-transcriptional it would make sense to have the necessary factors present in this way. In agreement with our results, genome-wide ChIP analysis of Rat1 revealed its presence over many gene bodies in addition to the vicinity of the poly(A) site (Kim *et al*, 2010). Furthermore, the exosome complex has also been linked to the transcription machinery in Drosophila (Andrulis *et al*, 2002). In both of these cases, cells were unperturbed in pre-mRNA processing indicating that exonucleases may ordinarily track with Pol II.

Degradation from the 5′ end of RNA requires a decapped substrate. Indeed, depletion of the decapping enzyme, Dcp2, stabilised some transcripts following SSA treatment. Although tagged Dcp2 was previously found predominantly in the cytoplasm, an endogenous population of nuclear Dcp2 has been observed consistent with our own ChIP and western blotting analysis (Liu *et al*, 2004). Moreover, budding yeast Dcp2 can shuttle between both compartments (Grousl *et al*, 2009). We find that Dcp2 is frequently not involved in pre-mRNA degradation upon SSA treatment implying the existence of other means of transcript decay. An additional decapping activity (Nudt16) was recently described in human cells; however this protein was originally reported to be cytoplasmic (Song *et al*, 2010) and may therefore be unlikely to perform this function. Finally, the Rat1 co-factor, Rai1, possesses decapping activity toward unmethylated caps (Jiao *et al*, 2010). Although decapping activity has not been tested for the human homologue, Dom3Z, we did not observe any effect of its depletion on degradation of aberrant β-globin RNA or on transcriptional termination (our unpublished observations).

Decapping is not the exclusive means of generating substrates for 5′→3′ degradation. Indeed, cleavage at the poly(A) site provides the best defined substrate for these enzymes (Kim *et al*, 2004; Gromak *et al*, 2006). It was recently shown that blocking the interaction between U1 snRNA and its pre-mRNA target activates processing of intronic poly(A) signals (Kaida *et al*, 2010). The authors also detected a small amount of cleavage product in SSA treated cells, which presumably would be a potential target for Xrn2. Cleavage of microRNA-containing introns by Drosha occurs co-transcriptionally (Morlando *et al*, 2008) as does cleavage of β-globin terminator region RNA (Dye and Proudfoot, 2001). Both of these activities have been shown to generate Xrn2 substrates (West *et al*, 2004; Ballarino *et al*, 2009). RNAse H cleavage of widespread R-loop structures (RNA:DNA hybrids) could also create entry sites for exonucleases given their 5′ phosphate termini (Mischo *et al*, 2011). Finally, the Dis3 subunit of the exosome possesses endonuclease activity (Lebreton *et al*, 2008), though we did not observe a significant effect of its depletion following SSA treatment (our unpublished observations). Thus, there may be a range of mechanisms that provide substrates to Xrn2. Endonucleolytic cleavage of pre-mRNA would also provide potential exosome substrates.

Our data indicate that transcripts must be efficiently retained at chromatin sites in order to be degraded by Xrn2. This is illustrated by comparing βglobin In1m transcripts, many of which are released, with ΔTIn1m transcripts that are not released. Although both produce a partially spliced β-globin transcript only those deriving from ΔTIn1m are degraded by Xrn2. Similarly, P27 pre-mRNAs are efficiently released into the nucleoplasm following SSA treatment and are not Xrn2 targets whereas six other pre-mRNAs are not released but are targeted by Xrn2 upon splicing inhibition. The determinants of whether aberrant transcripts are degraded by Xrn2 might be similar to those involved in releasing RNA from chromatin. These include lack of splicing, failure to assemble spliceosomes and inefficient 3′ end processing and Pol II termination (Dye *et al*, 2006; West *et al*, 2008; Martins *et al*, 2011).

It will be interesting to understand the reasons for the differential localisation of RNA following SSA treatment. It has been shown that, while splicing is prevented by SSA treatment, recruitment of snRNP's to genes is unaffected (Schmidt *et al*, 2011), which may allow the release of unprocessed RNA. In these instances Pol II might even terminate transcription, which is something that may also cause transcript release to be observed. The six transcripts

studied in detail here are much longer than those previously studied. Therefore, there is no opportunity to terminate transcription shortly after splicing failure and so no obvious means of releasing the RNA. Such circumstances likely preclude any nucleoplasmic accumulation and then increase the exposure of these RNAs to co-transcriptional degradation.

It is now established that most pre-mRNA processing occurs co-transcriptionally. The current study identifies a new function for Xrn2 in degrading aberrant pre-mRNA. It is also the first, to our knowledge, to provide strong evidence that degradation of many aberrant transcripts initiates co-transcriptionally.

Materials and methods

Primer sequences and siRNA target sites
See Supplementary Table 1.

Plasmids
The WT, In1m and pAm (previously called HIVβ, HIVβIVS1SAmut and HIVβp(A)mut) have been described (Dye and Proudfoot, 1999). The Tat plasmid required for trans-activation of the HIV promoter is also described (Adams *et al*, 1988) as is the EPO plasmid (West and Proudfoot, 2009). ΔTIn1m and ΔTpAm were constructed by ligation of a PCR product generated from amplification of In1m and pAm with the ΔTf and ΔTr primer pairs. The VA plasmid contains the adenovirus VAI gene and was a gift from Nick Proudfoot.

RNA isolation
Nuclear and cytoplasmic RNA fractionation was previously described (West and Proudfoot, 2008). Chromatin-associated and nucleoplasmic RNA was isolated using the protocol described in (Dye *et al*, 2006; Wuarin and Schibler, 1994). RNA was treated twice with Turbo DNase (Ambion). 1 μg of RNA was used for reverse transcription and was isolated from equivalent numbers of cells in each case. Fractionation and transfection efficiency was analysed by detection of co-transfection control VA or EPO RNA as well as endogenous GAPDH mRNA.

Chromatin and RNA immunoprecipitation
The ChIP and RIP protocol was based on a previously published ChIP protocol by (Glover-Cutter *et al*, 2008) with modifications detailed in our Supplementary Material.

Nuclear run on
Nuclear run on was based largely on the protocol in (Ashe *et al*, 1997) but with specific modifications to incorporate the use of 4-Thio UTP in place of ^{32}P-UTP (see Supplementary Material).

Northern Blotting
5–10 μg of total or fractionated RNA was resolved on a glyoxal gel. Following capilliary transfer, membranes were probed with a β-globin exon 3 probe made by PCR amplification of WT using Beta e3f/Betae3r primer pairs using a DECA prime kit (Ambion). The membrane was washed 2x in 1x SSPE, 0.1% SDS. Bands were visualised following exposure to a phosphor screen. For our detailed protocol see Supplementary Material.

Reverse transcription and PCR
1 μg RNA was reverse transcribed using Inprom II (Promega) and random hexamer primers. Parallel reactions were performed in the absence of reverse transcriptase. 1/20th of the cDNA mix was used for real-time PCR using 5–10 pmol of forward and reverse primer and Sensimix SYBR (Bioline) in a Qiagen Rotorgene machine. Students *t*-tests were performed to establish the significance (presented as *P*-values) of any important changes observed.

Cell culture
For transient transfections, a 50% confluent 6 cm dish of HeLa cells was transfected with 0.5 μg TAT, 3 μg reporter plasmid and 1 μg of VA and EPO plasmids for 4 h using Lipofectamine 2000 (Invitrogen). RNA was isolated the following day.

For RNAi, 30% confluent 6 cm dishes of cells were transfected with 18 μl 0.2 mM siRNA, using 4.8 μl Lipofectamine RNAiMAX (Invitrogen), following the manufacturers' guidelines. RNA or protein was isolated 48–72 h post-transfection. When plasmid transfections were performed in conjunction with RNAi, plasmids were transfected 48 h after the siRNA transfection and RNA analysed a further 24 h later. For SSA treatment, cells were grown in the presence of 100 ng/ml SSA for 3 h.

Bioinformatics
We used the data deposited by Kaida *et al*, 2010 (GEO accession: GSE24179) and identical search criteria. For transcript analysis we used the UCSC gene annotations and for genes we used the Ensembl gene 61 dataset.

Antibodies
4H8 (abcam ab5408), S2 (abcam 5095), hRrp6 (abcam), γ-tubulin (Sigma). Xrn2 ChIP and RIP was performed using Xrn2 antibodies from Bethyl Labs (A301-103A and A301-102A). Dcp2 ChIP experiments were performed using antibodies from Bethyl labs (A302-597A) or Sigma (D6319). The antibody used for Xrn2 Western analysis was a gift from Nick Proudfoot.

Protein fractionation and western blotting
Blots were probed with antibodies to detect Rrp6 (1:1000), Xrn2 (1:1000), γ Tubulin (1:2000), Histone H3 (1:2000) and Dcp2 (1:1000). Binding was detected with anti-rabbit (1:5000) or anti-mouse (1:5000), where appropriate using luminol reagents (Santa Cruz). Nuclear and cytoplasmic fractions were isolated as for RNA and nuclear extracts were treated in 100 μl RIPA buffer with 1 μl Benzonase (Sigma) for 30 mins at room temperature followed by a 10 min spin at 12000 × g.

Supplementary data
Supplementary data are available at *The EMBO Journal* Online (http://www.embojournal.org).

Acknowledgements

We would like to thank Minoru Yoshida (Riken Institute) for providing Spliceostatin A and Natasha Gromak and Nick Proudfoot for anti-Xrn2. This research was supported by a career development award from The Wellcome Trust (088499/Z/09/Z).

Author contributions: SW designed the experiments and wrote the paper. LD and SW performed and analysed the experiments. AK performed the bioinformatic analysis. We would also like to thank Aziz El Hage, Marie-Joelle Schmidt and Nick Proudfoot for reading the paper.

Conflict of interest

The authors declare that they have no conflict of interest.

References

Adams SE, Johnson ID, Braddock M, Kingsman AJ, Kingsman SM, Edwards RM (1988) Synthesis of a gene for the HIV transactivator protein TAT by a novel single stranded approach involving in vivo gap repair. *Nucleic Acids Res* **16:** 4287–4298

Andrulis ED, Werner J, Nazarian A, Erdjument-Bromage H, Tempst P, Lis JT (2002) The RNA processing exosome is linked to elongating RNA polymerase II in Drosophila. *Nature* **420:** 837–841

Ashe HL, Monks J, Wijgerde M, Fraser P, Proudfoot NJ (1997) Intergenic transcription and transinduction of the human beta-globin locus. *Genes Dev* **11:** 2494–2509

Ballarino M, Pagano F, Girardi E, Morlando M, Cacchiarelli D, Marchioni M, Proudfoot NJ, Bozzoni I (2009) Coupled RNA processing and transcription of intergenic primary microRNAs. *Mol Cell Biol* **29:** 5632–5638

Bentley DL (2005) Rules of engagement: co-transcriptional recruitment of pre-mRNA processing factors. *Curr Opin Cell Biol* **17:** 251–256

Bousquet-Antonelli C, Presutti C, Tollervey D (2000) Identification of a regulated pathway for nuclear pre-mRNA turnover. *Cell* **102:** 765–775

Brody Y, Neufeld N, Bieberstein N, Causse SZ, Bohnlein EM, Neugebauer KM, Darzacq X, Shav-Tal Y (2011) The in vivo kinetics of RNA polymerase II elongation during co-transcriptional splicing. *PLoS Biol* **9:** e1000573

Buratowski S (2009) Progression through the RNA polymerase II CTD cycle. *Mol Cell* **36:** 541–546

Corden JL (2007) Transcription. Seven ups the code. *Science* **318:** 1735–1736

Core LJ, Waterfall JJ, Lis JT (2008) Nascent RNA sequencing reveals widespread pausing and divergent initiation at human promoters. *Science* **322:** 1845–1848

Corrionero A, Minana B, Valcarcel J (2011) Reduced fidelity of branch point recognition and alternative splicing induced by the anti-tumor drug spliceostatin A. *Genes Dev* **25:** 445–459

Custodio N, Carmo-Fonseca M, Geraghty F, Pereira HS, Grosveld F, Antoniou M (1999) Inefficient processing impairs release of RNA from the site of transcription. *EMBO J* **18:** 2855–2866

de Almeida SF, Garcia-Sacristan A, Custodio N, Carmo-Fonseca M (2010) A link between nuclear RNA surveillance, the human exosome and RNA polymerase II transcriptional termination. *Nucleic Acids Res* **38:** 8015–8026

Dye MJ, Gromak N, Proudfoot NJ (2006) Exon tethering in transcription by RNA polymerase II. *Mol Cell* **21:** 849–859

Dye MJ, Proudfoot NJ (1999) Terminal exon definition occurs cotranscriptionally and promotes termination of RNA polymerase II. *Mol Cell* **3:** 371–378

Dye MJ, Proudfoot NJ (2001) Multiple transcript cleavage precedes polymerase release in termination by RNA polymerase II. *Cell* **105:** 669–681

Dziembowski A, Lorentzen E, Conti E, Seraphin B (2007) A single subunit, Dis3, is essentially responsible for yeast exosome core activity. *Nat Struct Mol Biol* **14:** 15–22

Eberle AB, Hessle V, Helbig R, Dantoft W, Gimber N, Visa N (2010) Splice-site mutations cause Rrp6-mediated nuclear retention of the unspliced RNAs and transcriptional down-regulation of the splicing-defective genes. *PLoS One* **5:** e11540

Egecioglu DE, Kawashima TR, Chanfreau GF (2011) *Quality control of MATa1 splicing and exon skipping by nuclear RNA degradation. Nucleic Acids Res*

El Hage A, Koper M, Kufel J, Tollervey D (2008) Efficient termination of transcription by RNA polymerase I requires the 5' exonuclease Rat1 in yeast. *Genes Dev* **22:** 1069–1081

Glover-Cutter K, Kim S, Espinosa J, Bentley DL (2008) RNA polymerase II pauses and associates with pre-mRNA processing factors at both ends of genes. *Nat Struct Mol Biol* **15:** 71–78

Gromak N, West S, Proudfoot NJ (2006) Pause sites promote transcriptional termination of mammalian RNA polymerase II. *Mol Cell Biol* **26:** 3986–3996

Grousl T, Ivanov P, Frydlova I, Vasicova P, Janda F, Vojtova J, Malinska K, Malcova I, Novakova L, Janoskova D, Valasek L, Hasek J (2009) Robust heat shock induces eIF2alpha-phosphorylation-independent assembly of stress granules containing eIF3 and 40S ribosomal subunits in budding yeast, Saccharomyces cerevisiae. *J Cell Sci* **122**(Pt 12): 2078–2088

Hessle V, Bjork P, Sokolowski M, Gonzalez de Valdivia E, Silverstein R, Artemenko K, Tyagi A, Maddalo G, Ilag L, Helbig R, Zubarev RA, Visa N (2009) The exosome associates cotranscriptionally with the nascent pre-mRNP through interactions with heterogeneous nuclear ribonucleoproteins. *Mol Biol Cell* **20:** 3459–3470

Hilleren P, McCarthy T, Rosbash M, Parker R, Jensen TH (2001) Quality control of mRNA 3'-end processing is linked to the nuclear exosome. *Nature* **413:** 538–542

Hilleren PJ, Parker R (2003) Cytoplasmic degradation of splice-defective pre-mRNAs and intermediates. *Mol Cell* **12:** 1453–1465

Jiao X, Xiang S, Oh C, Martin CE, Tong L, Kiledjian M (2010) *Identification of a quality-control mechanism for mRNA 5'-end capping. Nature*

Jimeno-Gonzalez S, Haaning LL, Malagon F, Jensen TH (2010) The yeast 5'-3' exonuclease Rat1p functions during transcription elongation by RNA polymerase II. *Mol Cell* **37:** 580–587

Kaida D, Berg MG, Younis I, Kasim M, Singh LN, Wan L, Dreyfuss G (2010) U1 snRNP protects pre-mRNAs from premature cleavage and polyadenylation. *Nature* **468:** 664–668

Kaida D, Motoyoshi H, Tashiro E, Nojima T, Hagiwara M, Ishigami K, Watanabe H, Kitahara T, Yoshida T, Nakajima H, Tani T, Horinouchi S, Yoshida M (2007) Spliceostatin A targets SF3b and inhibits both splicing and nuclear retention of pre-mRNA. *Nat Chem Biol* **3:** 576–583

Kaneko S, Rozenblatt-Rosen O, Meyerson M, Manley JL (2007) The multifunctional protein p54nrb/PSF recruits the exonuclease XRN2 to facilitate pre-mRNA 3' processing and transcription termination. *Genes Dev* **21:** 1779–1789

Kawauchi J, Mischo H, Braglia P, Rondon A, Proudfoot NJ (2008) Budding yeast RNA polymerases I and II employ parallel mechanisms of transcriptional termination. *Genes Dev* **22:** 1082–1092

Kim H, Erickson B, Luo W, Seward D, Graber JH, Pollock DD, Megee PC, Bentley DL (2010) Gene-specific RNA polymerase II phosphorylation and the CTD code. *Nat Struct Mol Biol* **17:** 1279–1286

Kim M, Krogan NJ, Vasiljeva L, Rando OJ, Nedea E, Greenblatt JF, Buratowski S (2004) The yeast Rat1 exonuclease promotes transcription termination by RNA polymerase II. *Nature* **432:** 517–522

Lebreton A, Tomecki R, Dziembowski A, Seraphin B (2008) Endonucleolytic RNA cleavage by a eukaryotic exosome. *Nature* **456:** 993–996

Listerman I, Sapra AK, Neugebauer KM (2006) Cotranscriptional coupling of splicing factor recruitment and precursor messenger RNA splicing in mammalian cells. *Nat Struct Mol Biol* **13:** 815–822

Liu SW, Jiao X, Liu H, Gu M, Lima CD, Kiledjian M (2004) Functional analysis of mRNA scavenger decapping enzymes. *RNA* **10:** 1412–1422

Luke B, Panza A, Redon S, Iglesias N, Li Z, Lingner J (2008) The Rat1p 5' to 3' exonuclease degrades telomeric repeat-containing RNA and promotes telomere elongation in Saccharomyces cerevisiae. *Mol Cell* **32:** 465–477

Mapendano CK, Lykke-Andersen S, Kjems J, Bertrand E, Jensen TH (2010) Crosstalk between mRNA 3' end processing and transcription initiation. *Mol Cell* **40:** 410–422

Martins SB, Rino J, Carvalho T, Carvalho C, Yoshida M, Klose JM, de Almeida SF, Carmo-Fonseca M (2011) Spliceosome assembly is coupled to RNA polymerase II dynamics at the 3' end of human genes. *Nat Struct Mol Biol* **18:** 1115–1123

McCracken S, Fong N, Yankulov K, Ballantyne S, Pan G, Greenblatt J, Patterson SD, Wickens M, Bentley DL (1997) The C-terminal domain of RNA polymerase II couples mRNA processing to transcription. *Nature* **385:** 357–361

Mischo HE, Gomez-Gonzalez B, Grzechnik P, Rondon AG, Wei W, Steinmetz L, Aguilera A, Proudfoot NJ (2011) Yeast Sen1 helicase protects the genome from transcription-associated instability. *Mol Cell* **41:** 21–32

Moore MJ, Proudfoot NJ (2009) Pre-mRNA processing reaches back to transcription and ahead to translation. *Cell* **136:** 688–700

Morlando M, Ballarino M, Gromak N, Pagano F, Bozzoni I, Proudfoot NJ (2008) Primary microRNA transcripts are processed co-transcriptionally. *Nat Struct Mol Biol* **15:** 902–909

Ozsolak F, Kapranov P, Foissac S, Kim SW, Fishilevich E, Monaghan AP, John B, Milos PM (2010) Comprehensive polyadenylation site maps in yeast and human reveal pervasive alternative polyadenylation. *Cell* **143:** 1018–1029

Roybal GA, Jurica MS (2010) Spliceostatin A inhibits spliceosome assembly subsequent to prespliceosome formation. *Nucleic Acids Res* **38:** 6664–6672

Schmid M, Jensen TH (2008) The exosome: a multipurpose RNA-decay machine. *Trends Biochem Sci* **33:** 501–510

Schmidt U, Basyuk E, Robert MC, Yoshida M, Villemin JP, Auboeuf D, Aitken S, Bertrand E (2011) Real-time imaging of cotranscriptional splicing reveals a kinetic model that reduces noise: implications for alternative splicing regulation. *J Cell Biol* **193:** 819–829

Schneider C, Leung E, Brown J, Tollervey D (2009) The N-terminal PIN domain of the exosome subunit Rrp44 harbors endonuclease activity and tethers Rrp44 to the yeast core exosome. *Nucleic Acids Res* **37:** 1127–1140

Schwer B, Shuman S (2011) Deciphering the RNA polymerase II CTD code in fission yeast. *Mol Cell* **43:** 311–318

Song MG, Li Y, Kiledjian M (2010) Multiple mRNA decapping enzymes in mammalian cells. *Mol Cell* **40:** 423–432

Stevens A, Maupin MK (1987) A 5′→3′ exoribonuclease of human placental nuclei: purification and substrate specificity. *Nucleic Acids Res* **15:** 695–708

Torchet C, Bousquet-Antonelli C, Milligan L, Thompson E, Kufel J, Tollervey D (2002) Processing of 3'-extended read-through transcripts by the exosome can generate functional mRNAs. *Mol Cell* **9:** 1285–1296

van Dijk E, Cougot N, Meyer S, Babajko S, Wahle E, Seraphin B (2002) Human Dcp2: a catalytically active mRNA decapping enzyme located in specific cytoplasmic structures. *EMBO J* **21:** 6915–6924

Wang ET, Sandberg R, Luo S, Khrebtukova I, Zhang L, Mayr C, Kingsmore SF, Schroth GP, Burge CB (2008) Alternative isoform regulation in human tissue transcriptomes. *Nature* **456:** 470–476

Wang M, Pestov DG (2010) 5'-end surveillance by Xrn2 acts as a shared mechanism for mammalian pre-rRNA maturation and decay. *Nucleic Acids Res* **39:** 1811–1822

West S, Gromak N, Proudfoot NJ (2004) Human 5′→3′ exonuclease Xrn2 promotes transcription termination at co-transcriptional cleavage sites. *Nature* **432:** 522–525

West S, Proudfoot NJ (2008) Human Pcf11 enhances degradation of RNA polymerase II-associated nascent RNA and transcriptional termination. *Nucleic Acids Res* **36:** 905–914

West S, Proudfoot NJ (2009) Transcriptional termination enhances protein expression in human cells. *Mol Cell* **33:** 354–364

West S, Proudfoot NJ, Dye MJ (2008) Molecular dissection of mammalian RNA polymerase II transcriptional termination. *Mol Cell* **29:** 600–610

Wuarin J, Schibler U (1994) Physical isolation of nascent RNA chains transcribed by RNA polymerase II: evidence for cotranscriptional splicing. *Mol Cell Biol* **14:** 7219–7225

